RESEARCH ON THERMOMECHANICAL STRESS OF LONG NOZZLE AND IMPROVEMENT MEASURES

Wang Zhigang, Associate Professor, Li Nan, Professor, Kong Jiangyi, Professor, Li Yourong, Professor, Wuhan University of Science and Technology, Wuhan, China, *wzgwy@126.com*

Abstract

Long nozzle is an important component for non-oxidating casting of steel. High stress in the neck of the long nozzle is a major cause of fracture of the neck. In this paper, the thermal and mechanical stresses were calculated by finite element method under working conditions and vibration normalized to the casting direction. Also, the influencing factors of thermal stress and decreasing stress measures have been studied. Calculation results indicate thermal stress is the main portion in total stress, and increasing the non-contact length on the inner-upper surface of the nozzle can decrease the stress in the neck effectively. Increasing the non-contact length can be accomplished by installing heat insulating material on the inner-upper surface or expanding the inner diameter of the nozzle.

Key words: long nozzle, thermomechanical stress, finite element, neck

1. INTRODUCTION

Recently, to improve the quality of the continuous casting pallet board, some techniques including non-oxidation casting, which can effectively prevent liquid steel from secondary oxidation and decrease impurities in the steel, have been adopted. In the non-oxidating casting technique, the long nozzle is an important component. However, high thermal stress, due to thermal impact and mechanical stress resulting from vibration of the long nozzle during casting, is often generated in the neck, which results in cracking, therefore, it is essential to study the thermomechanical stress of long nozzle under working conditions.

In this paper, using the finite element method, the thermal and mechanical stresses have been calculated. Also, the influencing factors of thermomechanical stress and decreasing stress measures have been studied. The results of this study may bring insight during the design of the long nozzle to minimize the damage in the neck.

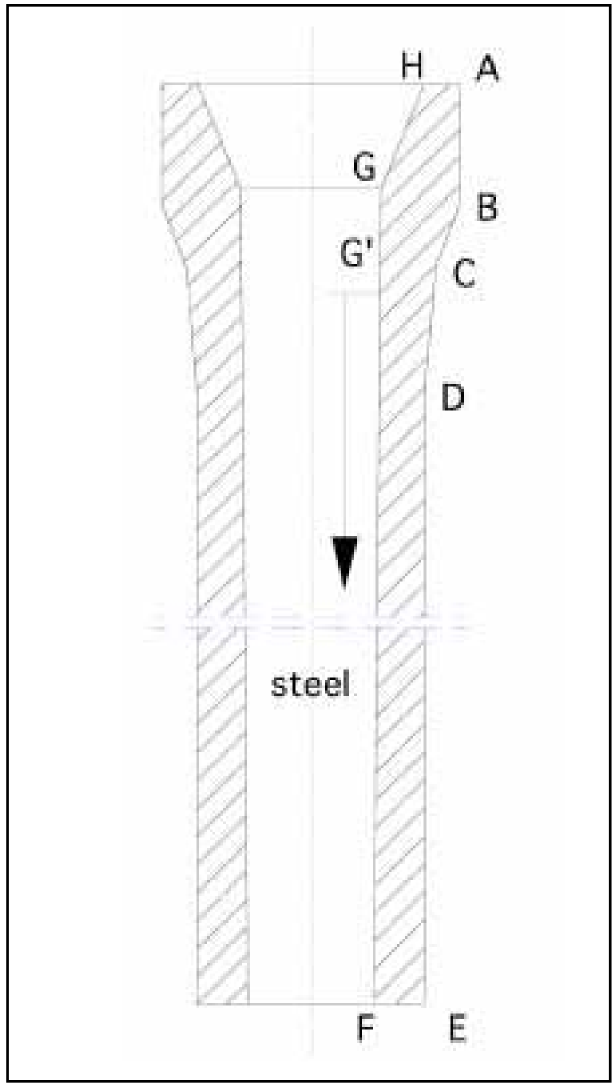

Figure 1. Section of long nozzle.

2. THERMAL STRESS AND ITS INFLUENCING FACTORS

2.1. Model for calculation

Figure 1 is the section illustration of the long nozzle. The geometrical modeling of the long nozzle employs a finite-element modeling technique. In FEM, when an object is symmetric in all respects (geometry, loads, constraints, and material properties), one can often take advantage of that fact to reduce the size and scope of the model. The long nozzle that displays geometric symmetry about the central axis is an axisymmetric structure, which may be represented in equivalent 2-D form. When only thermal stress is calculated, the long nozzle is symmetrical in all respects. Thus, a section of long nozzle is required for modeling. The material properties of long nozzle for calculation are listed in Table 1.

2.2. Thermal boundary conditions

During casting, the inner surface of the long nozzle (FG part in Figure 1) contacts the liquid steel while the outer surface of long nozzle (DE part in Figure 1) is air-cooled. Therefore, the temperature time dependent load is directly applied to the inner surface. In

Table 1. Material properties for calculation.

Thermal conductivity (w/m·K)	18.14
Specific heat (kJ/kg·K)	1.0
Bulk density (kg/m^3)	2350
Modulus of elasticity (GPa)	6.2
Poisson's ratio	0.15
Thermal expansion (%)	0.37

order to simulate the thermal impact during the beginning stage of casting, it is assumed that the temperature of the inner surface of the long nozzle increases sharply from the preheating temperature to the temperature 1530°C of molten steel in a short time, which is called thermal impact time, and then remains constant. On the other hand, the heat exchange between the long nozzle and atmosphere is convection whose coefficient is 58 w/m^2·K with the air temperature of 50°C.

2.3. Mechanical boundary condition

Since the long nozzle is fixed with the lower nozzle of ladle at the HG section in Figure 1 by the holding implement in the neck (BC part in Figure 1), the perpendicular directions of the HG and BC section are restricted in displacement when the thermal stress is calculated.

2.4. Influencing factors of thermal stress

2.4.1. Effect of thermal impact time

Thermal stress, which is generated in the long nozzle, is investigated at selected thermal impact times of 0s (temperature of inner surface increasing instantaneously to molten steel temperature at the start of casting), 3s, 5s and 10s. Because the neck is the stress concentration zone, the stress of D point in Figure 1 is selected to study the influence of the thermal impact time.

The peak values of axial and circumferential stress of D point and times of reaching peak values are listed in Table 2.

Based on the data shown in Table 2, it can be concluded that the thermal impact times barely change the peak stress no matter the axial or circumferential stress, but it can influence the time of reaching peak values. The longer the thermal impact time, the longer the time required for stresses to increase to the peak values.

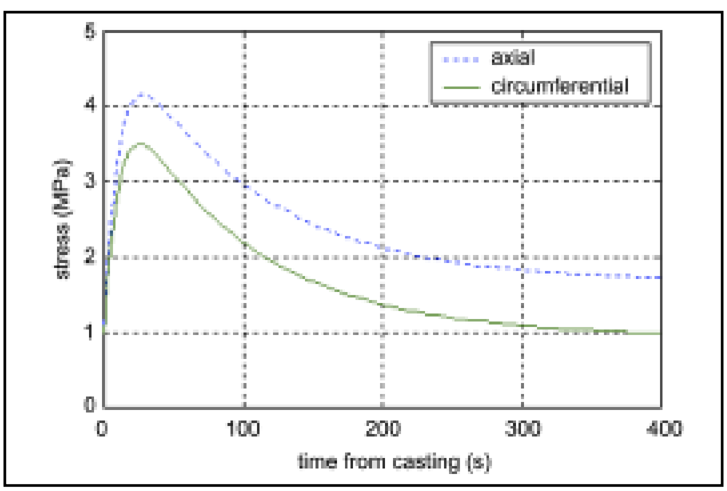

Figure 2. Stress variation at D point for an instantaneous increase from the preheat to the steel temperature (Zero-second thermal impact).

Table 2. Effect of different impact times.

Thermal impact time	Axial stress		Circumferential stress	
	time(s)	value (MPa)	time(s)	Value (MPa)
0	28.5	4.16	23.5	3.497
3	29.7	4.16	24.7	3.495
5	31.8	4.155	26.8	3.497
10	33.7	4.149	28.7	3.483

So, one can predict that the thermal impact time does not effect the calculation results when only the strength is considered, because the time of reaching peak stress does not determine the service life of the long nozzle.

Figure 2 is the stress variation of D point against time with the thermal impact time of 0 second. As shown in Figure 2, the stresses increase rapidly to the peaks, which are about 4.1 and 3.5 MPa for the axial and circumferential stress respectively, then decrease much slower and reach the steady-state values around 300s after casting. The steady-state value of the axial stress is about 1.72 MPa while the circumferential stress is about 1 MPa. It is obvious that the peak stresses due to thermal impact are 2 to 4 times steady-state stress. Some steps should be taken in decreasing its effect because it is harmful to the long nozzle.

2.4.2. Effect of preheating temperature

Generally, preheating is used for reducing thermal stress because it can decrease the temperature gradient throughout the long nozzle. The thermal stresses have been calculated using selected preheating temperatures of 30°C (no-preheating), 300°C, 600°C and 800°C. The peak stresses of D point with different preheating temperatures are listed in Table 3.

Compared with the thermal stress under no-preheating, the axial peak stress reduced 17.13%, 30.28%, 38.6% and the circumferential peak stress reduced 17.06%, 33.18%, 44.07% respectively with the preheating temperatures of 300°C, 600°C, 800°C. It can be concluded increasing the preheating temperature can reduce the influence of thermal impact effectively.

2.4.3. Effect of thermal conductivity

Using the same boundary conditions and preheating temperature (300°C), the thermal stresses have been calculated at selected thermal conductivity of 5 w/m·K, 18.14 w/m·K, 30 w/m·K and 50 w/m·K.

Figures 3 and 4 show the stress of D point varying with time for different thermal conductivity. From the two figures, one can find that all peak stresses, axial or circumferential, vary little with thermal conductivity, but the times of reaching peak values and steady-state stresses are related to it. The higher the thermal conductivity, the earlier the peak stresses appear, the shorter the stresses remain high and the more thermal impact the long nozzle withstands. In

Table 3. Effect of different preheating temperatures to the peak stress of D point (Zero-second thermal impact).

Preheating temperature °C	Axial stress (MPa)	Circumferential stress (MPa)
No-preheat	5.02	4.22
300	4.16	3.50
600	3.50	2.82
800	3.08	2.36

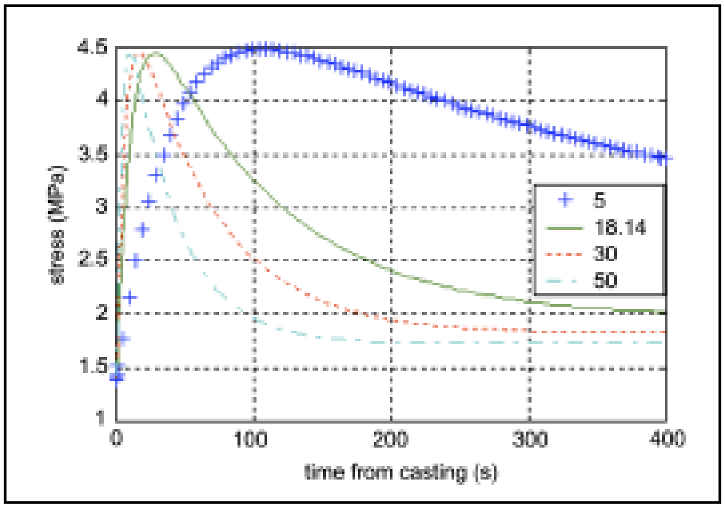

Figure 3. Axial stress of D point with different thermal conductivity.

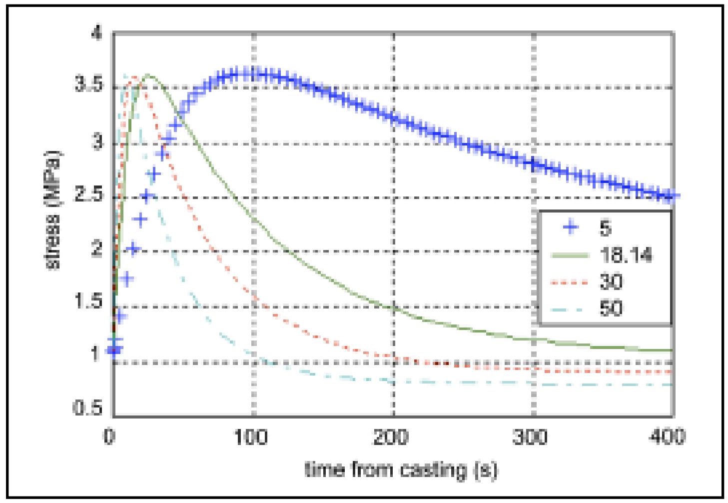

Figure 4. Circumferential stress of D point with different thermal conductivity.

this case, the long nozzle material must have the ability to resist heat shock.

The lower the thermal conductivity, the later the peak stresses appear, the longer the stresses remain high and the slower the stresses decrease with time. This requires the material of the long nozzle to have high strength. Therefore, the excellent anti-heat shock ability and high strength should be considered together when selecting thermal conductivity of the long nozzle. The calculation results show that the existing thermal conductivity (18.14 w/m·K) of the long nozzle is appropriate, because it is a compromise between the excellent anti-heat shock ability and high strength.

3. MECHANICAL STRESS UNDER VIBRATION

The upper part of long nozzle is fixed while the lower part is free under its working condition. During casting, the vibration generated is due to the impact of liquid steel flow to the inner surface, which creates high stress in the neck of the long nozzle. In order to simulate the effect of vibration, displacement is applied to the E point in Figure 1. Because the stress in the neck is proportional to the displacement, only the amplitude of displacement is considered to get the maximum stress.

Since the load from vibration is not symmetrical about the central axis but about a plane, a 3-D model of one half of the long nozzle is modeled using the finite element method.

The mechanical boundary conditions are similar to those used for calculating the thermal stress. Here, the HG and BC part in the 2-D model are used as turning surfaces formed by them in 3-D model for boundary conditions.

For different displacements of 3mm, 5mm and 6mm which are applied to the E point, the mechanical stresses resulting from vibration were calculated. Figure 5 shows the axial stress distribution with the displacement of 5mm. As shown in the figure, the maximum stress appears on the neck, which is 2.549 MPa. The maximum stresses are 1.53 MPa and 3.059 MPa respectively, while the displacements are 3 mm and 6 mm. It is obvious the maximum axial stress is proportional to the displacement applied to E point.

4. TOTAL STRESS

In order to study the influences of thermal and mechanical stresses on the total stress, the thermal and mechanical stresses have been calculated using the same boundary conditions described above, under the conditions that the preheating temperature is 300°C, thermal impact time is 3s and displacement of E point is 5 mm. Because the vibration mainly generates the axial stress and the axial stress resulting from thermal impact is higher than the circumferential stress, only the total axial stress is studied.

Figure 6 shows the variations of the thermal stress, mechanical stress and total stress with the distance from the neck of the long nozzle (CDE part in Figure 1), when the thermal stress in the neck reaches the peak. It is concluded that thermal stress is the main cause of cracking in the long nozzle, because the thermal stress is the major portion of the total stress while the mechanical stress under vibration is smaller.

5. MEASURES OF DECREASING STRESS

Because the mechanical stress distribution under vibration is not changed and if the installation style remains unchanged, only decreasing thermal stress or changing its distribution to avoid the peaks overlapping can reduce the total stress. In general, increasing the preheating temperature and changing the thermal boundary condition are the effective ways to reduce the total stress. The former has been described above. Here, the thermal boundary condition of the inner surface has been changed through modifying the length of the non-contact with the steel.

Using the same thermal boundary condition of the exterior surface, the thermal stress distributions have been calculated with the length of the non-contact with the steel (GG′ part in Figure 1) of 0, 20, 62, 85 and 124 mm.

5.1 Effect on stress distribution in space

Figure 7 and 8 show the variation of thermal stress with the distance from the neck along the exterior surface at the moment of stress in the neck reaching its peak. As shown in Figure 7 and 8, the position and value of peak total stress vary little with the length of non-contact stress with the steel, but the trends from the neck to the position of peak are different. There is a large zone, from the neck (C point) to the peak stress point, which almost equals the

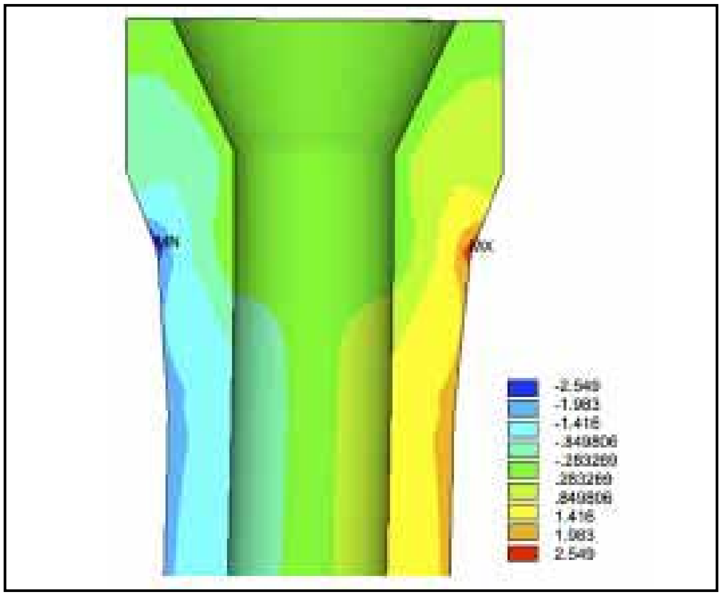

Figure 5. Axial stress distribution under vibration (5 mm).

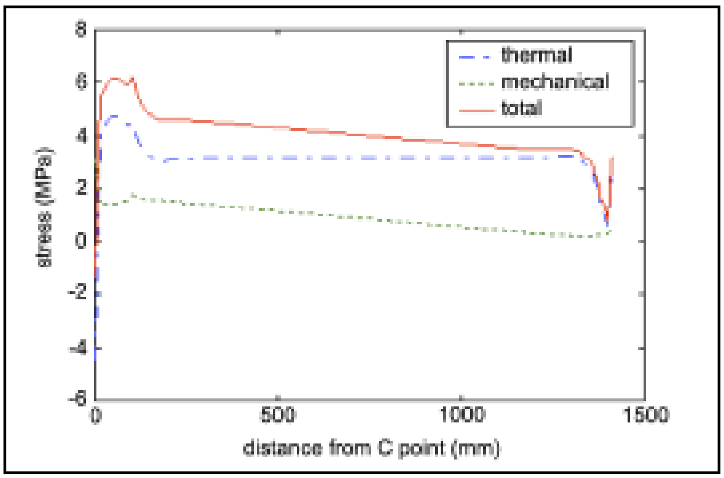

Figure 6. Stress on the exterior surface.

maximum if the length of non-contact with the steel is small; whereas, the thermal stress is high only in a small zone if the length is larger. Therefore, increasing the length of non-contact with the steel can effectively reduce the area of zone with high stress.

5.2 Effect on stress distribution in time

The variation of axial stress of D point with time is shown in Figure 9 for different lengths of non-contact with the steel. From the figure, one can find that the peak stresses are similar with different lengths, but the stress is high in a long time with the length of 0 and 20 mm while in a shorter time with the length of 62, 85 and 124 mm. Thus, increasing the length can decrease the time of the stress with a high value.

It is obvious that increasing the length of non-contact with the steel not only can reduce the area of the zone with high stress, but can also decrease the time of the stress with a high value. Increasing the non-contact length can be accomplished by installing heat insulating material on the inner-upper surface or extending the inner diameter of the nozzle.

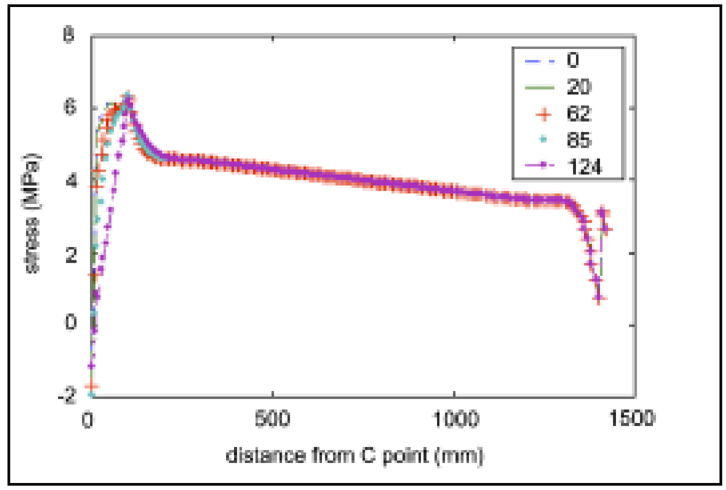

Figure 7. Stress on the exterior surface with different the length of non-contact with steel.

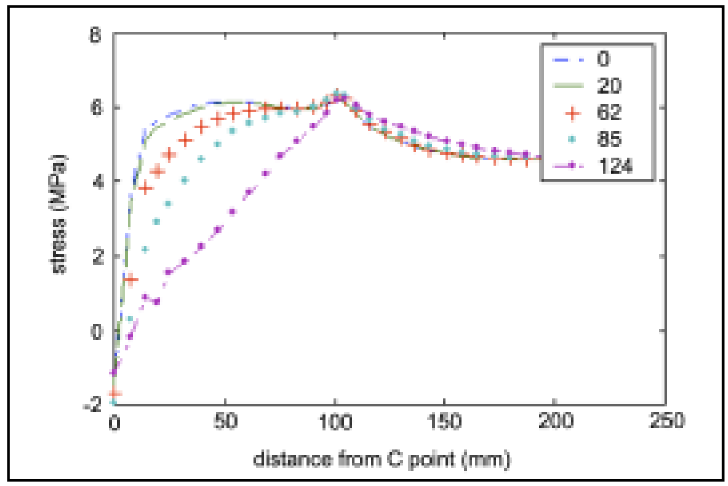

Figure 8. Enlarged drawing of Figure 7.

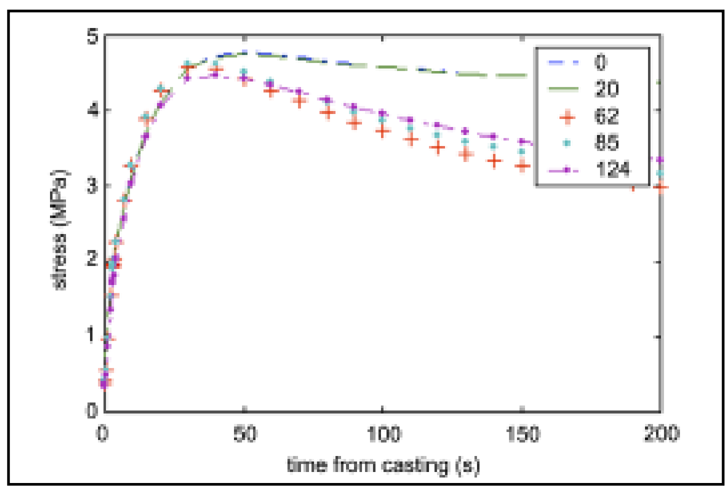

Figure 9. Stress of D point with different the length of non-contact with steel.

6. CONCLUSIONS

Using the finite element method, thermal stress under thermal impact and mechanical stress under vibration have been calculated.

Also the influencing factors of thermal stress and decreasing stress measures have been studied. The following conclusions are based on these results:

- thermal stress is the major portion of the total stress;
- time of thermal shock does not affect the peak stress;
- increasing preheating temperature can decrease the peak stress;
- different thermal conductivity of refractory can not change the value of peak stress but can change the rate of variation of stresses;
- increasing the non-contact length on the inner-upper surface of the nozzle can decrease the stress in the neck effectively;
- increasing the non-contact length can be accomplished by installing heat insulating material on inner-upper surface or extending inner diameter of the nozzle.

ACKNOWLEDGEMENTS

We would like to thank Hubei province key lab of ceramics and refractories for support of this work.

REFERENCES

1. R. Nakamura, S. Uchida, M. Yoshikawa, "3-D FEM Analysis for Long-nozzle Under Attachment Force and Vibration," Shinagawa technical report, 40 pp. 41-50 (1997).
2. C.A. Schacht, "Refractory Linings: Thermomechanical Design and Applications," Edited by Marcel Dekker Inc., NY (1995). RAN

Look for
Refractories Applications and News
on the web: www.ranews.info

The Bookshelf

Refractories Handbook by Charles A. Schacht (editor), Published by Marcel Dekker, Inc., 2004;

ISBN: 0-8247-5654-1.

This comprehensive reference details the technical, chemical, and mechanical aspects of high-temperature refractory composite materials for step-by-step guidance on the selection of the most appropriate system for specific manufacturing processes. The book surveys a wide range of lining system geometries and material combinations and covers a broad range of tests for the determination of the thermal, mechanical, strength, and resistance properties of refractories. With contributions from international specialists with widespread experience in the field, Refractories Handbook provides examples of refractory lining systems utilized in a range of industries, including glass, cement, and steel.

- Provides valuable recommendations on the design and installation of refractory lining systems
- Describes the most significant factors in castable lining design
- Provides examples of refractory lining systems utilized in a range of industries including petrochemical, glass, cement, and steel
- Considers the classification of load types, as well as issues related to refractories strength; compressive stress/strain data; arch, spherical, flat wall, and cylindrical lining behavior; and expansion allowance
- Highlights the latest developments in spinel-containing refractories and their application to steel, cement, and glass, manufacture
- Offers procedures to maximize the life of refractory lining systems
- Contains detailed descriptions of laboratory testing methods for evaluation of refractory properties

The book may be ordered from www.acers.org